

Electron Transport and Improved Confinement on Tore Supra

G. T. Hoang, C. Bourdelle, X. Garbet, T. Aniel, G. Giruzzi, M. Ottaviani.

Association EURATOM-CEA. CEA-Cadarache, 13108, St Paul-lez-Durance, France

W. Horton, P. Zhu

Institute for Fusion Studies, The University of Texas at Austin, Austin, Texas 78712, USA

R.V. Budny

Princeton Plasma Physics Laboratory, Princeton University, Princeton, NJ 08543, USA

e-mail: hoang@drfc.cad.cea.fr

Abstract

Magnetic shear is found to play an important role for triggering various improved confinement regimes through the electron channel. A wide database of hot electron plasmas ($T_e > 2 T_i$) heated by fast wave electron heating (FWEH) is analyzed for electron thermal transport. A critical gradient is clearly observed. It is found that the critical gradient linearly increases with the ratio between local magnetic shear (s) and safety factor (q). The Horton model, based on the electromagnetic turbulence driven by the electron temperature gradient (ETG) mode, is found to be a good candidate for electron transport modeling.

1. Introduction

Heat transport is usually analyzed in the regimes where the ion temperature (T_i) is larger than the electron temperature (T_e). Considerable progress has been made in understanding anomalous ion transport both experimentally and computationally. In contrast, the quasi-steady state plasmas ($20 - 120 \times \tau_E$) produced in Tore Supra with dominant electron heating provide an opportunity to study electron transport, a relevant issue for reactor-grade plasmas, dominated by α heating. These plasmas are heated by radio frequency (RF) power, either Lower Hybrid current drive (LHCD) or Ion Cyclotron Radio Frequency in H-minority (ICRH) and FWEH schemes, RF power up to 9.5 MW [1].

In this work, we try to clarify the physics underlying the electron thermal conductivity (χ_e) in the regimes with improved confinement seen on Tore Supra. In particular, we study the critical electron temperature gradient (∇T_e), and its parametric dependence. This paper is organized as follows. In Sec. 2, an overview of various improved confinement regimes with current profile (j) modification is presented. Electron transport analysis, particularly the determination of ∇T_e from both experimental results and theoretical approach, is reported in Sec. 3. In Sec. 4, a wide FWEH database is used for testing the model proposed by Horton

based on the turbulence driven by the electron temperature gradient (ETG) mode [2]. Finally, the conclusions are given in Sec. 5.

2. Improved confinement in current profile shaping experiments

Various improved confinement regimes were obtained by modification of the current profile.

These quasi-stationary plasmas exhibit an enhancement of stored energy, mainly through the electron channel, by a factor H up to 1.7 (Fig. 1). This figure shows five types of improved confinement regimes together with the standard L-mode. In these experiments, deuterium or helium plasmas are heated by different RF heating methods (LHCD, ICRH and FWEH).

i) *LHCD experiments*: LH waves are used to drive an off-axis non-inductive current in order to maintain a high magnetic shear in the gradient region (high- l_i) and at the same time a negative or low shear in the center (so-called Lower Hybrid Enhanced Performance, LHEP mode) [4]. In this configuration an H factor of 1.4 is achieved. In addition to the

improvement of global confinement, an electron internal transport barrier (ITB) appears when the central magnetic shear vanishes. This regime has been extended to steady state of 2 minutes in Tore Supra [5].

ii) *FWEH experiments*: The electron energy of these hot electron plasmas systematically exceeds the reference L-mode discharges by a factor up to 2.2, and the thermal energy confinement time is found to exceed the L-mode by a factor H of 1.7 [6]. The main mechanism of this improvement is the increase of s in the pressure gradient region, which is due to the high bootstrap current mainly induced by the electron temperature gradient.

iii) *Combined H-minority heating and fast current ramp-up*: in these plasmas, the electron ITB is sustained by application of the ICRH on the non-monotonic q -profile target preformed by a fast ramp-up [7]. It was found that the ITB is triggered mainly by negative magnetic

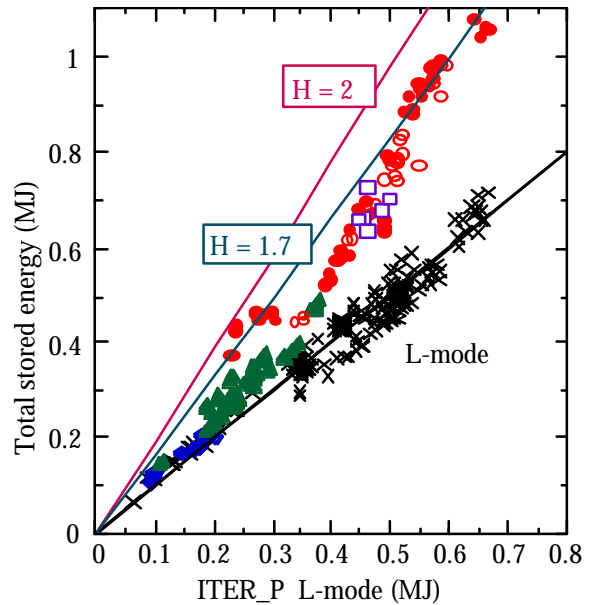


Fig. 1: Comparison of stored thermal energy of various discharges with ITER prediction for L-mode (circles: D/He H-minority heating; squares: combined H-minority heating with fast current ramp-up; triangles: FWEH; diamonds: LHCD; crosses: L-mode with LHCD).

shear, then maintained by ExB shear stabilizing effect when the current profile relaxes to the monotonic profile (low s). An H factor of 1.4-1.5 was obtained in this experiment.

iv) *High H-minority concentration heating experiments* [8, 9]: the confinement time of these discharges improves, reaching a value close to ELMy H-mode prediction. One of the main features of this type of discharge is the increase of s in the confinement region. Moreover, the central toroidal rotation increases and changes in the direction: from counter-current to co-current, correlated with the improved confinement. Very similar results are also observed in ALCATOR C-MOD [10].

Note that the confinement improves in both ion and electron channels in experiments (iii) and iv). In contrast, only the electron confinement improves in experiments (i) and (ii).

A significant reduction of density fluctuations was recorded in both configurations a) when the s profile is reversed or flat (low s) in the center [11]; b) increase of s in the confinement zone [6]. Heat transport analysis of the above regimes indicates a reduction, correlated with changing magnetic shear. Two examples are shown in Fig. 2 (experiment (iii)) and Fig. 3 (experiment (iv)). It appears that the electron transport coefficient (χ_e) significantly drops in the region where s is modified.

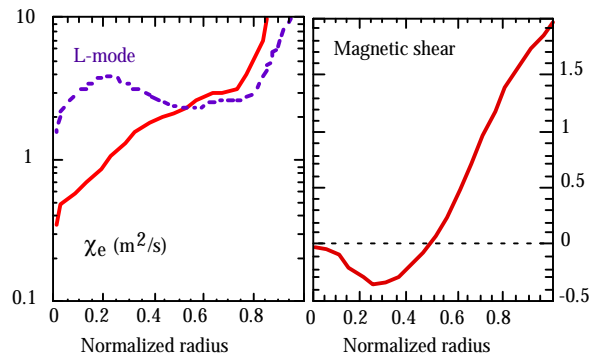


Fig. 2: Correlation between electron transport reduction (left) and central negative magnetic shear (right). Dashed curves: L-mode.

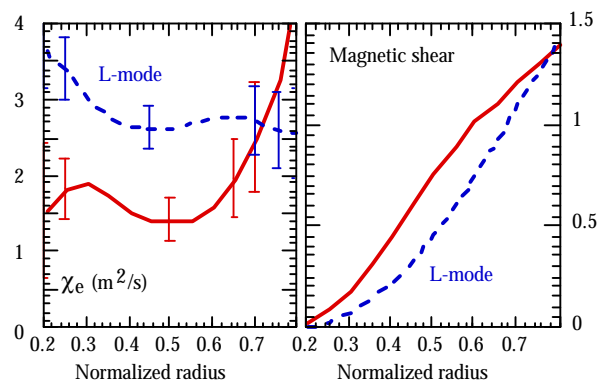


Fig. 3: Correlation between electron transport reduction (left) and increase of magnetic shear (right) in the gradient region.

3. Electron transport analysis

In previous work, transport analysis in Ref. [6] and both the density [12] and magnetic [13] fluctuations indicated an existence of ∇T_c in plasmas heated by LHCD or ICRH. In this work we investigate to the experimental determination of this critical electron temperature threshold. Especially, the magnetic shear dependence is studied to clarify the role of the q -profile in the improved confinement, observed in different configurations described in Sec. 2.

For this study, we use a limited data set of ^4He plasmas heated by fast wave, carefully chosen in order to obtain similar plasma parameters. The FWEH scenario was chosen either without any ion cyclotron resonance layer in the plasma or minimizing the parasitic damping of the ions in order to maximize the absorption of the wave by the electrons [1]. The FW power (P_{FW}) is therefore directly absorbed by the electrons, which implies that no fast particles were present in these discharges. The FW power deposition profile, computed with the codes ALCYON [14] and PION [15], is exponentially localized inside $r/a = 0.4$ and more than 90% of P_{FW} is absorbed by the electrons. These hot electron plasmas ($T_e > 2T_i$) are characterized by negligible electron-ion collisional coupling ($< 5\%$ of P_{FW}). They all have the same density (n_e) and q-profiles ($n_e(0) = 6 \times 10^{19} \text{ m}^{-3} \pm 10\%$, $q_{\text{edge}} = 4.4 \pm 5\%$) and were obtained at plasma current $I_p = 0.65 \text{ MA}$, toroidal field $B = 2.2 \text{ T}$ and $P_{\text{FW}} = 1.5 - 7.4 \text{ MW}$; 18 time slices over 8 discharges were selected. A power balance analysis of this set of discharges clearly shows the existence of a critical electron temperature gradient, as illustrated in Fig. 4, where the electron heat flux (Φ_e) is plotted versus $\nabla T_e / T_e$. We limit our analysis to normalized radii (r/a) between 0.2 and 0.7, since the plasma center is dominated by the heating source and the edge temperature measurements are affected by large uncertainties. For each radial position, the variations ($< 10\%$) of n_e and q are weaker than their absolute error bars. Here, the q profiles are measured by polarimetry with a systematic error in the range of 10% (at mid-radius) and 25% (in the center). The relative error of T_e (28 radial points measured by Thomson scattering and ECE diagnostics) is less than 20%. Since the electron-ion equipartition is negligible, the electron heat flux is determined within the error bar of 5%. A linear best fit gives the critical threshold $(\nabla T_e / T_e)_c$ ranging from 2 m^{-1} (in the center) to 6 m^{-1} (at the edge); its radial profile is shown in Fig. 5.

Stability analysis of these discharges also suggests the existence of a critical gradient threshold. This analysis has been done with a linear electrostatic gyro-kinetic code [16] in which both passing and trapped electrons and ions (ITG, ETG, and TEM modes) are taken into account. The results are in reasonable agreement with the power balance analyses. In Fig. 6, the maximum growth rates, over each spectrum at a given radial position, versus $\nabla T_e / T_e$ is reported together with the electron heat flux. The critical values $(\nabla T_e / T_e)_c$ deduced from the calculation of the linear electrostatic growth rates are lower than the values obtained from the power balance analysis (Fig. 7). One of the possible explanations could be expected from difference between the electrostatic and the electromagnetic thresholds. Indeed, previous experimental observations [12, 13] suggest that the anomalous heat transport of electrons is induced by electromagnetic turbulence on Tore Supra, while in our stability analysis we evaluate the threshold with an electrostatic model.

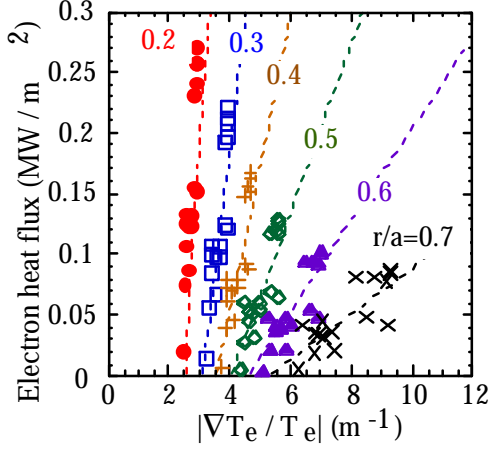


Fig. 4: Electron heat flux versus $\tilde{N}T_e / T_e$. Each symbol corresponds to a fixed radial position ($r/a = 0.2 - 0.7$).

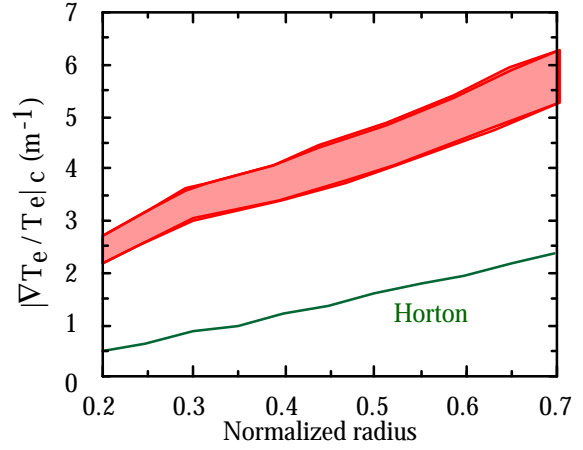


Fig. 5: Radial profile of $(\tilde{N}T_e / T_e)_c$, obtained from a linear fit of the experimental data in Fig. 4. Line: Horton's formula given in Eq. 2

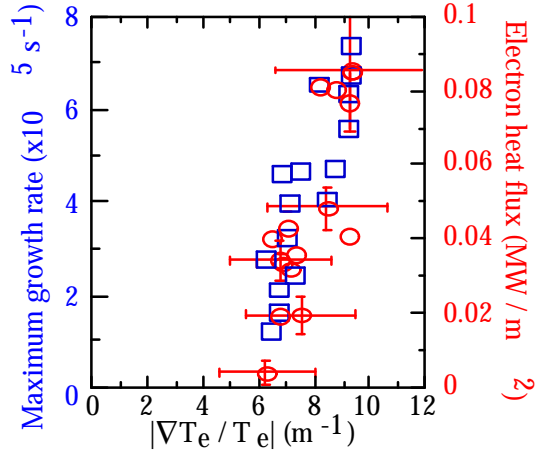
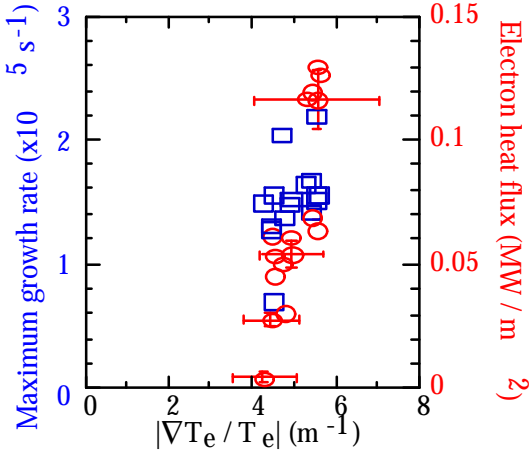


Fig. 6: Maximum linear growth rates (squares) and electron heat flux (circles) and versus $\tilde{N}T_e / T_e$, at $r/a = 0.5$ (left) and $r/a = 0.7$ (right).

The parametric dependence of the critical threshold was studied, showing a good correlation with the ratio s/q . From both power balance and stability analyses, $(\nabla T_e / T_e)_c$ is found to increase with s/q . The dimensionless parameter $[R \cdot (\nabla T_e / T_e)_c]$, deduced from both methods, is plotted versus s/q in Fig. 7 ($R = 2.28$ m, being the major radius). A best fit of the data from the power balance analysis gives an offset linear formula: $R \cdot (\frac{\nabla T_e}{T_e})_c = 5 + 10 \frac{s}{q}$. This is

consistent with the improvement of the confinement observed in high magnetic shear discharges. Here, we only explore the domain of positive magnetic shear, but the dependence of the threshold with s/q could be similar for negative magnetic shear, since the stability calculation predicts that the threshold increases with $|s/q|$, as shown in Fig. 8. This calculation has been done at mid-radius by varying s , and keeping the other parameters ($q, \nabla T_e, \nabla n_e$) constant. In Fig. 8, the masked area approximately illustrates the limit of validity of the code for weak values of s . Thus, we are not able to explain the low s improved

confinement regime. However, it is possible that the electron critical threshold increases when s is close to zero, as for the ion threshold predicted in global simulations of the ITG and TEM modes [17],

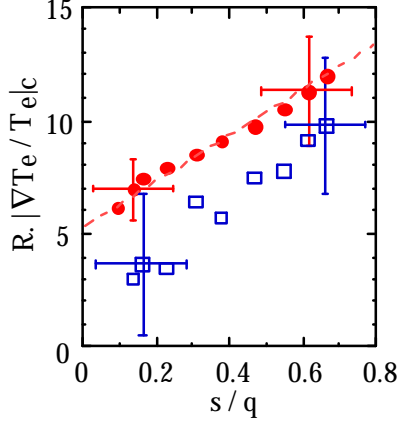


Fig. 7: Dimensionless parameter $R \cdot (\tilde{N}T_e / T_e)_c$ from power balance (circles; dashed curve: fit) and stability (squares) analyses versus s/q .

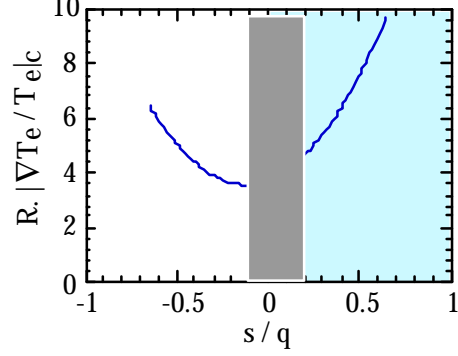


Fig. 8: Variation of $R \cdot (\tilde{N}T_e / T_e)_c$ with the ratio s/q , predicted by stability simulation with a linear electrostatic gyro-kinetic code at mid-radius. Masked area (s close to 0) illustrates the limit of validity of the code.

4. Comparison of transport models against the database

In Ref [6], two electron transport models, Bohm-like Taroni [18] and offset-linear Rebut-Lallia-Watkins (RLW) [19], have been tested against the Tore Supra results. It was found that these models could simulate the experimental results with some restrictions. The Taroni's model cannot reproduce the magnetic shear effect and exhibits a disagreement in electron temperature gradient dependence ($\nabla T_e > 4 \text{ keV/m}$). In contrast, the anomalous transport term in RLW model reproduces the temperature gradient and magnetic shear effect better. On the other hand, the parametric dependences of the critical gradient (Eq. 3), obtained from a fit of the JET data, are inaccurate. In a recent work [20], the electron thermal conductivity from the power balance analysis was tested against the model proposed by Horton. This model, based on the electromagnetic turbulence driven by ETG and collisionless electron skin depth [2], predicts the electron transport of FWEH discharges in Tore Supra well. χ_e is given by:

$$\chi_e^{\text{em}} = C_{\text{em}} q \frac{v}{\omega_{\text{pe}}^2} \frac{c^2}{(L_{T_e} R)^{1/2}} \left(-\nabla T_e - \nabla T_c^{\text{Hor}} \right) \quad (\text{Eq. 1})$$

$$\text{Where } \nabla T_c^{\text{Hor}} = 1.88 \left(\frac{|s| T_e}{qR} \right) \left(1 + Z_{\text{eff}} \frac{T_e}{T_i} \right) \quad (\text{Eq. 2})$$

Statistical analysis in Ref [20] indicates a weak dependence on q ($v \approx 0$), and C_{em} around 0.1. In Eq. 2, one can see that the Horton's formula predicts the same dependence on s/q of the critical threshold found in the experimental result. However, the absolute value of $(\nabla T_e / T_e)_c$

given by Eq. 2 is lower than the experimental value (Fig. 7). This can be explained by the fact that the constant in Eq. 2 (1.88) was chosen according to the ITG mode.

For comparison, we plot in Fig. 9 the electron heat flux predicted by three above models versus $(\nabla T_e / T_e)$ together with the data. This figure suggests that the electron transport in Tore Supra discharges is gyro-Bohm. Furthermore, the Horton model exhibits a good quality for modeling of FWEH discharges in Tore Supra. Fig. 9 also indicates that the threshold using in the Horton model, is too low. Simulation by multiplying Eq. 2 by a factor of 2 is in better agreement.

Above the critical threshold, electron transport is found to increase strongly with $\nabla T_e / T_e$. It could be reproduced by either an offset-linear or a strong power fit.

Assuming that χ_e is written in the following form

$$\chi_e \propto T_e^{5/2} \left(1 - \frac{(\nabla T_e / T_e)_c}{(\nabla T_e / T_e)} \right)^\alpha \left(\frac{\nabla T_e}{T_e} \right)^\alpha$$

Thus, above the threshold, the normalized heat flux, defined as $\frac{\Phi_e}{(n_e T_e^{5/2})}$, is proportional to

$\left(\frac{\nabla T_e}{T_e} \right)^{\alpha+1}$. Power fit of this quantity gives a value of α about 3 (Fig. 10). This result from

the power balance analysis is consistent with the experimental observations of the variation of $\nabla T_e / T_e$ as a function of T_e . $\nabla T_e / T_e$ varies approximately as $T_e^{-0.5}$, as shown in Fig. 11.

5. Conclusions

In summary, a critical electron temperature gradient is clearly shown to exist in Tore Supra hot electron plasmas. The critical threshold is found to increase with the ratio s / q . This result confirms the important role of s in the improved confinement discharges (H up to 1.7) on Tore Supra by increasing s in the confinement zone (high- l_i regime).

A comparison with the Horton's ETG model indicates that the experimental value is almost twice higher than the theoretical one. However, the Horton's formula reproduces the radial profile of the experimental threshold well.

Above the critical threshold, the electron heat transport strongly increases with $\nabla T_e / T_e$, approximately as $(\nabla T_e / T_e)^3$. This could be the reason why many models, with offset-linear

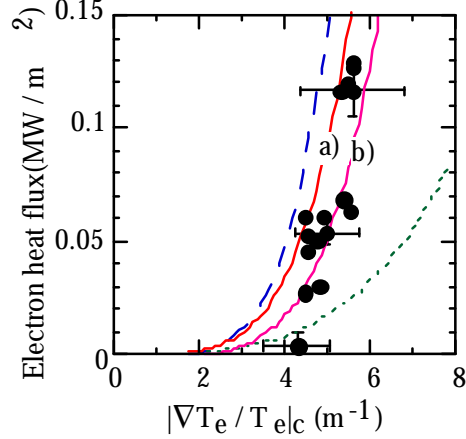


Fig. 9: Electron heat flux versus $\tilde{\nabla} T_e / T_e$, at mid-radius, compared with the models: RLW (dashed), Taroni (dot), and Horton (full): a) critical threshold given in Eq. 2; b) Eq. 2 multiplied by 2.

or strong power dependence ∇T_e , can simulate electron transport with acceptable discrepancies when the temperature gradient exceeds the critical value. In spite of its low predicted critical threshold, the Horton's model based on the electromagnetic turbulence appears to be a good candidate for electron transport modeling.

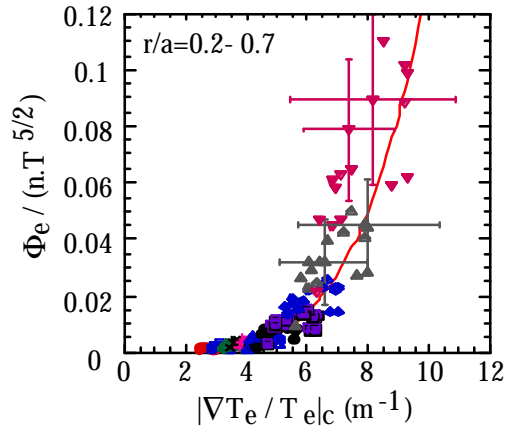


Fig. 10: Normalized heat flux versus $\tilde{\nabla}T_e / T_e$.
Full curve: fit $\mu (\tilde{\nabla}T_e / T_e)^{3.85}$. ($P = 1.5 - 7.4$ MW).

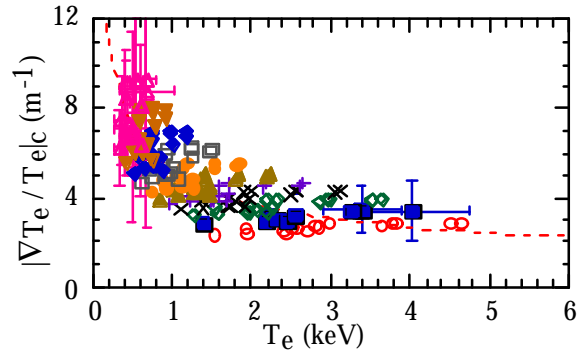


Fig. 11: Variation of $\tilde{\nabla}T_e / T_e$ with T_e : $\mu T_e^{-0.49}$ from a best fit (dashed line).

Acknowledgements

The diligent support of the Tore Supra team is gratefully acknowledged. The authors would also like to thank Dr. F. Ryter from ASDEX for fruitful discussions.

- [1] Equipe Tore Supra, Plasma Phys. Control. Fusion **36 Suppl.** (1994) B123.
- [2] W. Horton, Rev. of Mod. Phys. **71** (1999) 735.
- [3] S.M. Kaye, et al., Nucl. Fusion **37** (1997) 1303.
- [4] G.T. Hoang, et al., Nucl. Fusion **34** (1994) 75.
- [5] Equipe Tore Supra Plasma Phys. Control. Fusion **38** (1996) A251.
- [6] G.T. Hoang, al., Nucl. Fusion **38** (1998) 117.
- [7] G.T. Hoang, al., Physical Rev. Lett. **84** (2000) 4593.
- [8] G.T. Hoang, et al., Nucl. Fusion **40** (2000) 913.
- [9] L-G Eriksson, G.T. Hoang, V. Bergeaud, submitted to Nucl. Fusion.
- [10] J.E. Rice, et al., Nucl. Fusion **38** (1998) 75.
- [11] G. Antar, et al., submitted to Physics of Plasmas.
- [12] P. Devynck, et al., Plasma Phys. Control. Fusion **39** (1997) 1355.
- [13] L. Colas, et al., Nucl. Fusion **38** (1998) 903.
- [14] A.Bécoulet, et al., Physics of Plasmas **1** (1994) 2908.
- [15] L.-G. Eriksson, et al., Nucl. Fusion **33** (1993) 1037.
- [16] C. Bourdelle, et al., 27th Eur. Conf. Budapest, 2000, submitted to Physics of Plasmas.
- [17] X. Garbet, et al., US-European TTF workshop, Varenna (2000).
- [18] A. Taroni et al., in Controlled Fusion and Plasma Physics (Proc. 20th Eur. Conf. Lisbon, 1993) **17C, Part I**, European Physical Society, Geneva (1993) 87.
- [19] P.H. Rebut, et al., Phys. Fluids **B3** (1991) 2209.
- [20] W. Horton, et al., Physics of Plasmas **7** (2000) 1494.